purpura—hemolytic uremic syndrome. *Semin Hematol* 2004;**41**:68-74.

[21] Uchida T, Wada H, Mizutani M, Iwashita M, Ishihara H, Shibano T, et al. Identification of novel mutations in ADAMTS13 in an adult patient with congenital thrombotic thrombocytopenic purpura. *Blood* 2004;**104**:2081-3.

[22] Kokame K, Matsumoto M, Fujimura Y, Miyata T. VWF73, a region from D1596 to R1668 of von Willebrand factor, provides a minimal substrate for ADAMTS-13. *Blood* 2004; **103**:607-12.

[23] Mannucci PM, Capoferri C, Canciani MT. Plasma levels of von Willebrand factor regulate ADAMTS-13, its major cleaving protease. *Br J Haematol* 2004;**126**:213-8.

[24] Rougier N, Kazatchkine MD, Rougier JP, Fremeaux-Bacchi V, Blouin J, Deschenes G, et al. Human complement factor H deficiency associated with hemolytic uremic syndrome. *J Am Soc Nephrol* 1998;**9**:2318-26.

[25] Noris M, Brioschi S, Caprioli J, Todeschini M, Bresin E, Porrati F, et al. International Registry of Recurrent and Familial HUS/TTP: Familial haemolytic uraemic syndrome and an MCP mutation. *Lancet* 2003;**362**:1542-7.

[26] Park YD, Yoshioka A, Kawa K, Ishizashi H, Yagi H, Yamamoto Y, et al. Impaired activity of plasma von Willebrand factor-cleaving protease may predict the occurrence of hepatic veno-occlusive disease after stem cell transplantation. *Bone Marrow Transplant* 2002;**29**:789-94.

TR-03024; No of Pages 6
Thrombosis Research (2006) xx, xxx-xxx

ELSEVIER

THROMBOSIS RESEARCH

intl.elsevierhealth.com/journals/thre

BRIEF COMMUNICATION

Quantitative Western blot analysis of plasma ADAMTS13 antigen in patients with Upshaw-Schulman syndrome

Hiromichi Ishizashi[a], Hideo Yagi[a], Masanori Matsumoto[a], Kenji Soejima[b], Tomohiro Nakagaki[b], Yoshihiro Fujimura[a,*]

[a] *Department of Health Science and Blood Transfusion Medicine, Nara Medical University, Nara 634-8522, Japan*
[b] *First Research Department, The Chemo-Sero-Therapeutic Research Institute, Kumamoto 869-1298, Japan*

Received 17 May 2006; received in revised form 19 July 2006; accepted 31 July 2006

KEYWORDS
ADAMTS13;
Antigen;
USS;
TTP

Upshaw-Schulman syndrome (USS) was originally reported as a disease complex, characterized by chronic thrombocytopenia and hemolytic anemia, that was dramatically improved by infusions of fresh frozen plasma (FFP) [1-6]. USS is now known to be a hereditary deficiency in the activity of von Willebrand factor-cleaving protease (VWF-CP), also known as ADAMTS13 (a disintegrin-like and metalloproteinase with thrombospondin type 1 motifs 13), and lacks ADAMTS13 autoantibodies (inhibitors) [7]. In contrast, acquired deficiency of ADAMTS13 activity caused by inhibitors is defined as thrombotic thrombocytopenic purpura (TTP), a life-threatening generalized disease characterized by Moschcowitz's pentad [8,9]. Thus, USS is alternatively called congenital TTP, and genetic analysis of *ADAMTS13* has revealed that its mutations are present across the entire gene and not in hot spots [7,10-15]. The *ADAMTS13* gene is located on chromosome 9q34 and USS is a recessive disease, so most USS patients are genetically compound heterozygotes or homozygotes. When expressed in mammalian cells, the *ADAMTS13* gene mutants found in USS patients showed deficient ADAMTS13 activity (ADAMTS13:ACT) that was induced by disturbing the synthesis and/or secretion of the protease. However, these results were left unchecked in the patient plasmas. It was recently shown that the normal plasma level of ADAMTS13 antigen (ADAMTS13:AGN) is approximately 1 μg/ml, according to a sandwich enzyme-linked immunosorbent assay (ELISA) using polyclonal or monoclonal antibodies (mAbs) against ADAMTS13. USS patients exhibit severely reduced levels of ADAMTS13:AGN, resulting in reduced levels of ADAMTS13:ACT [16,17]. However, the investigation of the ADAMTS13 molecules in these patients has not yet been perfomed *in vivo*.

We therefore analyzed plasma ADAMTS13:AGN in 9 USS patients and their 25 family members, in

* Corresponding author. Department of Blood Transfusion Medicine, Nara Medical University, 840 Shijyo-cho, Kashihara City, Nara 634-8522, Japan. Tel.: +81 744 22 3051x3289; fax: +81 744 29 0771.
E-mail address: yfujimur@naramed-u.ac.jp (Y. Fujimura).

0049-3848/$ - see front matter © 2006 Published by Elsevier Ltd.
doi:10.1016/j.thromres.2006.07.012

Please cite this article as: Hiromichi Ishizashi et al., Quantitative Western blot analysis of plasma ADAMTS13 antigen in patients with Upshaw-Schulman syndrome, Thrombosis Research (2006), doi:10.1016/j.thromres.2006.07.012.

whom *ADAMTS13* gene mutations were identified by Western blot (WB) using an anti-ADAMTS13 mAb, WH2-11-1. The epitope of this mAb resides on the 4th thrombospondin-1 domain and is reactive by WB under both reducing and non-reducing conditions [18].

Materials and methods

Assays for ADAMTS13:ACT and ADAMTS13 inhibitors

ADAMTS13:ACT and titers of ADAMTS13 inhibitors (ADAMTS13:INH) were assayed by a novel, highly-sensitive ELISA using a murine mAb (N10-146) specifically recognizing Tyr1605 residue of VWF-A2 domain, generated by ADAMTS13 cleavage, and a recombinant GST-VWF73-His polypeptide as a substrate [19,20]. This ELISA had a limit of detection of 0.5% of the normal ADAMTS13:ACT level in normal pooled plasma, and the average plasma level of ADAMTS13:ACT was 99.1±43.0% (mean±2SD). Inhibitor titers were expressed as Bethesda units (BU), where one inhibitor unit is defined as the amount necessary to reduce ADAMTS13:ACT levels to 50% of the normal levels. Titers of >0.1 BU/ml, as measured by the novel ELISA, were considered significant [20].

Patients

Nine patients from 9 different families (Families A-I) with histories of USS were enrolled in our study. For each family, diagnoses were confirmed by identifying the *ADAMTS13* gene mutations responsible for the disease, as previously described [10,14,15,21]. Of the 25 USS relatives we tested, 23 were definite carriers and 2 were normal subjects.

Citrated plasma samples taken from USS patients were frozen in aliquots at −80 °C until use. For controls, normal citrated plasma was obtained from 60 healthy individuals (30 females and 30 males, aged 20-40 years) and kept in aliquots at −80 °C. Pooled normal plasma was used as the control standard for this study. These studies were conducted with the approval of the Nara Medical University ethics committee.

Characterization of the murine anti-ADAMTS13 mAb WH2-11-1

A murine anti-ADAMTS13 mAb, termed WH2-11-1 (IgG1-κ), was produced by the Chemo-Sero-Therapeutic Research Institute (Kumamoto, Japan) using recombinant (r) full-lengh ADAMTS13 as the immunogen [18]. Monoclonal IgGs were purified on a Protein A column (Amersham Biosciences, NJ, USA) according to the manufacturer's instructions. WH2-11-1 recognizes an epitope on the 4th thrombospondin-1 domain, and this was verified using C-terminal truncated rADAMTS13. This mAb detected plasma ADAMTS13:AGN as a 170-kD band by WB under non-reducing conditions and a single 190-kD band under reducing conditions. However, this mAb showed no significant inhibition of ADAMTS13:ACT. In some WB analyses under non-reducing conditions, another anti-ADAMTS13 mAb with an epitope on the disintegrin domain, A10, was also used [22].

Analysis of plasma ADAMTS13:AGN

We quantified plasma ADAMTS13:AGN by WB. Two microliters of undiluted or diluted plasma samples per lane were analyzed after treatment with sample buffer containing SDS and β-mercaptoethanol, followed by separation by reducing 5% SDS polyacrylamide gel electrophoresis (SDS-PAGE). After electrophoresis, proteins were blotted onto polyvinylidene difluoride (PVDF) microporous membranes (Immobilon-P, Millipore, MA, USA) using cyclohexylaminopropanesulfonic acid (CAPS)-NaOH buffer (pH11) [23]. We probed the blots for ADAMTS13:AGN with WH2-11-1 as the primary mAb, followed by secondary staining with horseradish peroxidase (HRP)-conjugated goat anti-mouse IgG (Kirkegaaed and Perry Lab, Gaithersburg, MO). After incubation with Western Lighting Chemiluminescence Reagent (PerkinElmer Life Sciences, Shelton, CT), the blots were exposed to X-ray film. Densitometric analysis of ADAMTS13:AGN was performed for the 190-kD band using NIH imageJ (developed by the National Institutes of Health, http://rsb.info.nih.gov/nih-image/).

Results

When diluted normal plasma was analyzed by WB under reducing conditions, WH2-11-1 detected a single 190-kD band of ADAMTS13:AGN, and the detection limit was determined to be 3% of the normal controls (Fig. 1, top). Densitometric analysis of the 190-kD band showed a nearly straight line on a semi-logarithmic graph (data not shown). Using this assay, the normal range of ADAMTS13:AGN in 60 healthy Japanese subjects (30 females and 30 males, aged 20-4 years) was determined to be 101.6±49.4% (mean±2SD).

Next, plasma from 9 USS patients and 25 of their relatives (23 definite carriers and 2 normal subjects), whose *ADAMTS13* gene mutations had been identified (Table 1), were analyzed using this method. It was noteworthy that before analysis, 7

Please cite this article as: Hiromichi Ishizashi et al., Quantitative Western blot analysis of plasma ADAMTS13 antigen in patients with Upshaw-Schulman syndrome, Thrombosis Research (2006), doi:10.1016/j.thromres.2006.07.012.

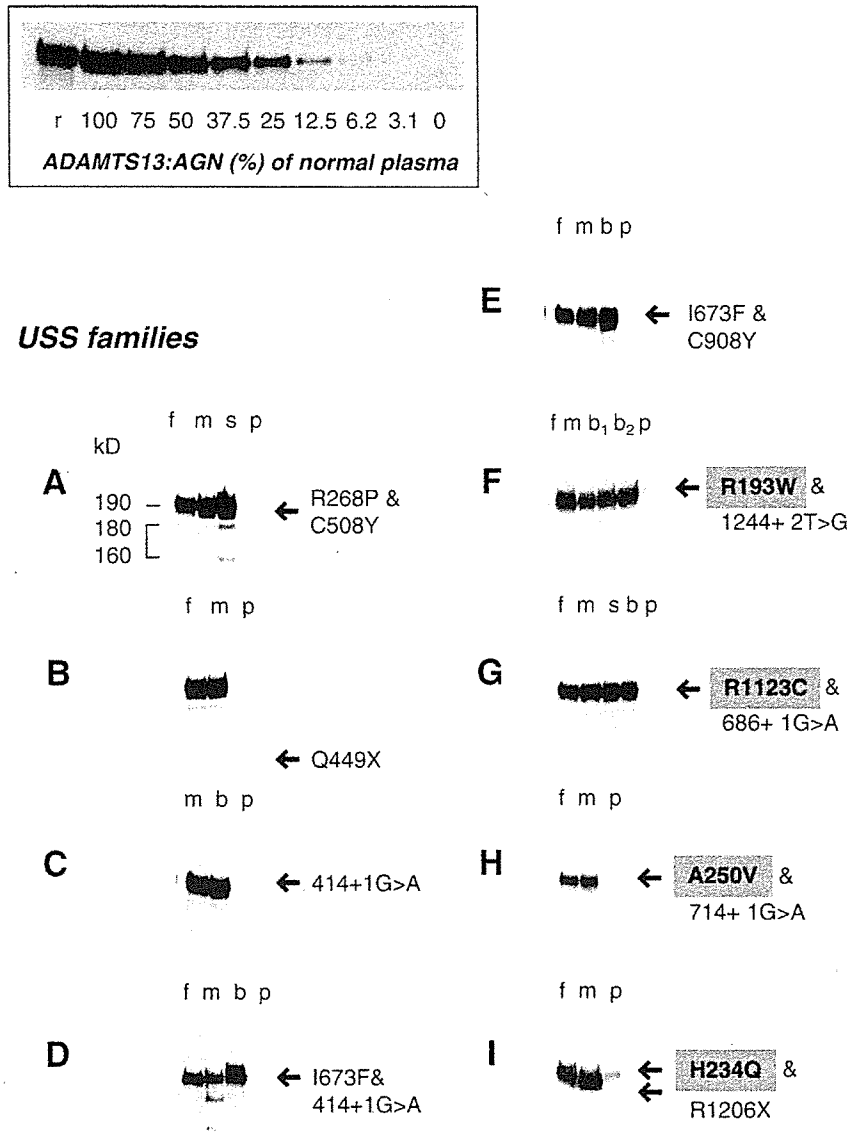

Figure 1 WB analysis under reducing conditions of plasma ADAMTS13:AGN in 9 families with a history of USS. WB analysis of plasma ADAMTS13:AGN in the members of the nine USS families are shown: f (father), m (mother), b(brother), s (sister), and p (patient). Under reducing conditions, recombinant (r) and/or plasma-derived ADAMTS13 from normal individuals is detected as a 190-kD band using an anti-ADAMTS13 mAb, WH2-11-1. Based on serial dilutions of normal plasma, the detection limit was determined to be 3% of the normal controls (top). The 190-kD band is completely absent from the plasma of 5 USS patients (A-E), but faintly detectable in the plasma of 4 patients (F-I) with *ADAMTS13* gene mutations (R193W, R1123C, A250V, and H234Q). Furthermore, several 180-160-kD bands are visible in certain family members under reducing conditions (bottom).

of the 9 USS patients had undetectable levels (<0.5% of the normal control) of plasma ADAMTS13:ACT, while the remaining 2 (patients F and H) showed low but appreciable activities (0.8% and 0.6%) according to a sensitive ADAMTS13:ACT-ELISA. By WB, four missense mutations (R268S, C508Y, I673F, and C908Y) and one intron 4 mutation (414+1G>A) resulted in no appreciable ADAMTS13:AGN in the plasma. Furthermore, one nonsense mutation (Q449X) resulted in the protein being secreted into the culture medium (as a C-terminally truncated 50-kD protein in *in vitro* studies), and this mutant was not detectable in plasma, even with a mAb (A10) directed to the disintegrin domain (data not shown). With regard to another nonsense mutation, R1206X, *in vitro* expression studies have not been done, but the current study has shown that the R1206X mutant protein is absent from patients' plasma.

Please cite this article as: Hiromichi Ishizashi et al., Quantitative Western blot analysis of plasma ADAMTS13 antigen in patients with Upshaw-Schulman syndrome, Thrombosis Research (2006), doi:10.1016/j.thromres.2006.07.012.

t1.1 **Table 1** Plasma levels of ADAMTS13:ACT and AGN in patients with USS and its relatives, whose *ADAMTS13* gene mutations were identified

t1.2
t1.3

USS families	ADAMTS13 gene mutations	ADAMTS13: ACT(%) by ELISA	ADAMTS13: AGN(%) by WB	ADAMTS13: ACT/AGN ratio
A				
f	R268P/P475S	4.2	37	0.11
m	C508Y/WT	18	48	0.38
s	P475S/WT	52	80	0.65
p	R268P/C508Y	<0.5	<3	*
B				
f	Q449X/WT	37	37	1.00
m	Q449X/WT	48	48	1.00
p	Q449X/Q449X	<0.5	<3	*
C				
m	414+1G>A/WT	34	46	0.74
b	414+1G>A/WT	41	44	0.93
p	414+1G>A/414+1G>A	<0.5	<3	*
D				
f	I673F/WT	40	40	1.00
m	414+1G>A/WT	40	30	1.33
b	414+1G>A/WT	31	50	0.62
p	414+1G>A/I673F	<0.5	<3	*
E				
f	I673F/WT	20	35	0.57
m	C908Y/WT	33	50	0.66
b	WT/WT	32	67	0.48
p	I673F/C908Y	<0.5	<3	*
F				
f	R193W/WT	17	40	0.43
m	1244+2T>G/WT	10	35	0.29
b1	1244+2T>G/WT	37	48	0.77
b2	WT/WT	50	54	0.93
p	R193W/1244+2T>G	0.8	5	0.16
G				
f	R1123C/WT	32	40	0.80
m	686+1G>A/WT	43	58	0.74
s	686+1G>A/WT	38	62	0.61
b	R1123C/WT	34	64	0.53
p	686+1G>A/R1123C	<0.5	4	*
H				
f	A250V/WT	18	16	1.13
m	714+1G>A/WT	20	23	0.87
p	714+1G>A/A250V	0.6	4	0.15
I				
f	H234Q/WT	24	40	0.60
m	R1206X/WT	18	36	0.50
p	H234Q/R1206X	0.5	6	*
	Normal individuals (mean±2SD)	99.1±43.0	101.6±49.4	

t1.48 f: father, m: mother, b: brother, s: sister, p: patient.

In contrast, the 190-kD band was present for four missense mutations (R193W, R1123C, A250V, and H234Q), but to a much lesser extent than in the normal controls. In addition, in two family members of A-s and D-m, two additional bands at 180 and 160 kD were intensified (Fig. 1).

The results of the densitometric analyses of the plasma levels of the 190-kD ADAMTS13:AGN are summarized in Table 1. Four USS patients had 4-6% antigen, five had less than 3%. The definite carriers of USS ($n=23$) revealed levels of 43.8±13.7%. We also examined the association of ADAMTS13:ACT (X axis) and ADAMTS13:AGN (Y axis) for both the USS patients and the definite carriers. We found a significant positive correlation between these two values ($Y=1.08X+9.1$, $r^2=0.74$, $p<0.01$) (data not shown).

Discussion

A number of *ADAMTS13* gene mutations have been reported in patients with USS or congenital TTP, but only a limited number of these mutations have been analyzed by gene expression studies using HeLa or HEK293 cells. During our initial studies in HeLa cells,

Please cite this article as: Hiromichi Ishizashi et al., Quantitative Western blot analysis of plasma ADAMTS13 antigen in patients with Upshaw-Schulman syndrome, Thrombosis Research (2006), doi:10.1016/j.thromres.2006.07.012.

we observed that *ADAMTS13* with a nonsense mutation, Q449X (found in USS family B), was secreted into the culture medium as a C-terminally truncated 50-kD protein. However, we have shown here that it is not present in plasma. The cause of this discrepancy is not entirely clear, but we presume that the 50-kD protein is more sensitive to proteolytic degradation *in vivo*. The mechanism of proteolytic regulation of ADAMTS13 in normal circulation has not been elucidated, but Crawley et al. showed that three serine proteinases (thrombin, Xa, and plasmin), which are ubiquitously involved in normal hemostasis, cleave ADAMTS13:AGN *in vitro*, leading to a concomitant decrease in ADAMTS13:ACT [24]. Thus, it is reasonable to assume that a proteolytic mechanism might be involved in the rapid clearance of the 50-kD protein from circulation. Furthermore, certain missense mutations (R193W and A250V) led to moderate secretion inhibition [14,15], and other missense mutations of the *ADAMTS13* gene (R268S, C508Y, I673F, and R1123C) showed an almost total lack of secretion despite normal production within cells, suggesting a disturbance of the secretion mechanism in these variants [10,14]. The results presented here largely agree with those obtained from *in vitro* experiments, and in fact USS patients F and H (R193W and A250V) showed a less intense but distinct 190-kD band by WB under reducing conditions. By directly analyzing patient plasma in this study, we have demonstrated that both the missense mutations R1123C and H234Q produce proteins present in circulation but to a much lesser extent than the controls. On the other hand, the protein by nonsense mutation R1206X was not present as a C-terminally truncated protein. These results suggested that R1123C and H234Q mutations might lead to secretion inhibition and the R1206X mutation might show proteolytic clearance. Concerns regarding the potentially increased *in vivo* proteolysis of these ADAMTS13 mutants are important, and should be explored in detail in future studies. In addition, the 23 USS carriers had plasma levels of ADAMTS13:AGN as lower than 50% of normal controls, and these values correlated well with the ADAMTS13:ACT measured in these carriers. In general, the levels of both ADAMTS13:ACT and :AGN in the carriers' plasma therefore appear to reflect the function of a single wild-type allele.

In conclusion, the analysis of plasma ADAMTS13:AGN, as demonstrated here, represents a useful diagnostic tool for USS patients. Further investigation of ADAMTS13:AGN and its mutations in USS would contribute to our understanding of *ADAMTS13 gene* function, and could aid the development of new therapeutic approaches.

Acknowledgements

We thank Ms. Ayami Isonishi and Hitomi Nishimura for excellent technical assistance. This work was supported by grants-in-aid for scientific research (Nos. 15591017 and H17-02 to Dr. Fujimura; 16590796 and H17-005 to Dr. Matsumoto; 17500439 to Dr. Ishizashi) from the Japanese Ministry of Education, Culture and Science and from the Ministry of Health and Welfare of Japan for Blood Coagulation Abnormalities.

References

[1] Schulman I, Pierce M, Likens A, Currimbhoy Z. Studies on thrombopoiesis: I. A factor in normal human plasma required for platelet production: chronic thrombocytopenia due to its deficiency. *Blood* 1960;**14**:947-57.

[2] Upshaw JD. Congenital deficiency of a factor in normal plasma that reverses microangiopathic hemolysis and thrombocytopenia. *N Engl J Med* 1978;**298**:1350-2.

[3] Furlan M, Robles R, Solenthaler M, Wassmer M, Sandoz P, Lämmle B. Deficient activity of von Willebrand factor-cleaving protease in chronic relapsing thrombotic thrombocytopenic purpura. *Blood* 1997;**89**:3097-103.

[4] Häbele J, Kwehrel B, Ritter J, Jürgens H, Lämmle B, Furlan M. New strategies in diagnosis and treatment of thrombotic thrombocytopenic purpura: case report and review. *Eur J Pediatr* 1999;**158**:883-7.

[5] Kinoshita S, Yoshioka A, Park Y-D, Ishizashi H, Konno M, Funado M, et al. Upshaw-Schulman syndrome revisited: a concept of congenital thrombotic thrombocytopenic purpura. *Int J Hematol* 2001;**78**:101-8.

[6] Barbot J, Costa E, Guerra M, Barreirinho MS, Isvarlal P, Robles R, et al. Ten years of prophylactic treatment with fresh-frozen plasma in a child with chronic relapsing thrombotic thrombocytopenic purpura as a result of a congenital deficiency of von Willebrand factor-cleaving protease. *Br J Haematol* 2001;**113**:649-51.

[7] Levy GG, Nichols WC, Lian EC, Foroud T, McClintick JN, McGee BM, et al. Mutations in a member of the ADAMTS gene family cause thrombotic thrombocytopenic purpura. *Nature* 2001;**413**:488-94.

[8] Moschcowitz E. Hyaline thrombosis of the terminal arterioles and capillaries; a hitherto undescribed disease. *Proc NY Pathol Soc* 1924;**24**:21-4.

[9] Amorosi EL, Ultmann JE. Thrombotic thrombocytopenic purpura: report of 16 cases and review of the literature. *Medicine* 1966;**45**:139-59.

[10] Kokame K, Matsumoto M, Soejima K, Yagi H, Ishizashi H, Funato M, et al. Mutations and common polymorphisms in *ADAMTS13* gene responsible for von Willebrand factor-cleaving protease activity. *Proc Natl Acad Sci U S A* 2002;**99**:11902-7.

[11] Schneppenheim R, Budde U, Oyen F, Angerhaus D, Aumann V, Drewke E, et al. von Willebrand factor cleaving protease and ADAMTS13 mutations in childhood TTP. *Blood* 2003;**101**:1845-50.

[12] Savasan S, Lee SK, Ginsburg D, Tsai HM. ADAMTS13 gene mutations in congenital thrombotic thrombocytopenic purpura with previously reported normal VWF cleaving protease activity. *Blood* 2003;**101**:4449-51.

[13] Antoine G, Zimmermann K, Plaimauer B, Grillowitzer M, Studt JD, Lämmle B, et al. ADAMTS13 gene defects in two

Please cite this article as: Hiromichi Ishizashi et al., Quantitative Western blot analysis of plasma ADAMTS13 antigen in patients with Upshaw-Schulman syndrome, Thrombosis Research (2006), doi:10.1016/j.thromres.2006.07.012.

brothers with constitutional thrombotic thrombocytopenic purpura and normalozation of von Willebrand factor-cleaving protease activity by recombinant human ADAMTS13. *Br J Haematol* 2003;**120:**821-4.

[14] Matsumoto M, Kokame K, Soejima K, Miura M, Hayashi S, Fujii Y, et al. Molecular characterization of *ADAMTS13* gene mutations in Japanese patients with Upshaw-Schulman syndrome. *Blood* 2004;**103:**1305-10.

[15] Uchida T, Wada H, Mizutani M, Iwashita M, Ishihara H, Shibata T, et al. Identification of novel mutations in ADAMTS13 in an adult patient with congenital thrombotic thrombocytopenic purpura. *Blood* 2004;**104:**2081-3.

[16] Rieger M, Ferrari S, Kremer Hovinga JA, Konetschny C, Herzog A, Koller L, et al. Relationship between ADAMTS13 activity and ADAMTS13 antigen levels in healthy donors and patients with thrombotic microangiopathies (TMA). *Thromb Haemost* 2006;**95:**212-20.

[17] Feys HB, Liu F, Dong N, Pareyn I, Vauterin S, Vandeputte N, et al. ADAMTS-13 plasma level determination uncovers antigen absence in acquired thrombotic thrombocytopenic purpura and ethnic differences. *J Thromb Haemost* 2006;**4:**955-62.

[18] Soejima K, Nakamura H, Hiroshima M, Morikawa W, Nozaki C, Nakagaki T. Analysis on the molecular species and concentration of circulating ADAMTS13 in blood. *J Biochem* 2006;**139:**147-54.

[19] Kokame K, Matsumoto M, Fujimura Y, Miyata T. VWF73, a region from D1596 to R1668 of von Willebrand factor, provides a minimal substrate for ADAMTS-13. *Blood* 2004;**103:**607-12.

[20] Kato S, Matsumoto M, Matsuyama T, Isonishi A, Hiura H, Fujimura Y Novel monoclonal antibody-based enzyme immunoassay for determining plasma levels of ADAMTS13 activity. *Transfusion.* in press.

[21] Shibagaki Y, Matsumoto M, Kokame K, Ohba S, Miyata T, Fujimura Y, et al. Novel compound heterozygote mutations (H234Q/R1206X) of the ADAMTS13 gene in an adult patient with Upshaw-Schulman syndrome showing predominant episodes of repeated acute nenal failure. *Nephrol Dial Transplant* 2006;**21:**1289-92.

[22] Uemura M, Tatsumi K, Matsumoto M, Fujimoto M, Matsuyama T, Ishikawa M, et al. Localization of ADAMTS13 to the stellate cells of human liver. *Blood* 2005;**106:**922-4.

[23] Matsudaira P. Sequence from picomole quantities of proteins electroblotted onto polyvinylidene diffluoride membranes. *J Biol Chem* 1987;**262:**10035-8.

[24] Crawley JTB, Lam JK, Rance JB, Mollica LR, O'Donnell JS, Lane DA. Proteolytic inactivation of ADAMTS13 by thrombin and plasmin. *Blood* 2005;**105:**1085-93.

Please cite this article as: Hiromichi Ishizashi et al., Quantitative Western blot analysis of plasma ADAMTS13 antigen in patients with Upshaw-Schulman syndrome, Thrombosis Research (2006), doi:10.1016/j.thromres.2006.07.012.

Journal of Thrombosis and Haemostasis, 4: 177–185

ORIGINAL ARTICLE

Fatal thrombosis of antithrombin-deficient mice is rescued differently in the heart and liver by intercrossing with low tissue factor mice

M. HAYASHI,* T. MATSUSHITA,† N. MACKMAN,‡ M. ITO,§ T. ADACHI,† A. KATSUMI,† K. YAMAMOTO,¶ K. TAKESHITA,* T. KOJIMA,** H. SAITO,†† T. MUROHARA* and T. NAOE†

**Department of Cardiology, Nagoya University Graduate School of Medicine; †Department of Hematology, Nagoya University Graduate School of Medicine; ‡Department of Immunology and Cell Biology, The Scripps Research Institute; §Department of Pathology, Nagoya University Hospital; ¶Department of Blood Transfusion Service, Nagoya University Hospital; **Department of Medical Technology, Nagoya University School of Health Sciences; and ††Nagoya Medical Center, Honshu, Japan*

To cite this article: Hayashi M, Matsushita T, Mackman N, Ito M, Adachi T, Katsumi A, Yamamoto K, Takeshita K, Kojima T, Saito H, Murohara T, Naoe T. Fatal thrombosis of antithrombin-deficient mice is rescued differently in the heart and liver by intercrossing with low tissue factor mice. *J Thromb Haemost* 2006; **4**: 177–85.

Summary. *Background:* We previously reported that the targeted disruption of murine antithrombin (AT) gene resulted in embryonic lethality before 16.5 gestational days (gd) because of severe cardiac and hepatic thrombosis. *Objective and Methods:* To investigate the influences of lowered tissue factor (TF) activity upon hypercoagulation of $AT^{-/-}$ embryos, we crossed $AT^{+/-}$ with low TF ($mTF^{-/-}hTF^{+}$) mice to yield homozygous AT-deficient mice with the extremely low TF activity, that is expressed from the inserted human TF mini gene. *Results:* $AT^{-/-}$ embryos either with 50% TF ($AT^{-/-}mTF^{+/-}hTF^{+}$) or with low (~1% TF, $AT^{-/-}mTF^{-/-}hTF^{+}$) were not born, although the survival was prolonged until 18.5 gd. In both genotypes, histological examination showed disseminated thrombosis in hepatic sinusoidal space or in the portal veins, suggesting that the thrombogenesis caused loss of hepatic blood flow. As in original $AT^{-/-}$, $AT^{-/-}mTF^{+/-}hTF^{+}$ showed subcutaneous (s.c.) bleeding and also suffered from the myocardial degeneration apparently because of coronary thrombus formation. However, $AT^{-/-}mTF^{-/-}hTF^{+}$ had no skin hemorrhage and the thrombosis and degeneration were completely abolished in the heart. Myocardium of adult low TF mice had exhibited fibrosis secondary to hemorrhage; however, it was significantly decreased in low TF mice with $AT^{+/-}$. *Conclusions:* Our current model suggests that, in the heart, TF plays an important role in the thrombogenesis and it counterbalances AT-dependent anticoagulation. AT may be a potent anticoagulant during mice development and the activation and subsequent regulation of TF-procoagulant activity take place differently between the liver and the heart. These differences appear to point to local regulatory mechanisms in murine hemostasis.

Keywords: antithrombin, genetically altered mice, tissue factor.

Correspondence: Tadashi Matsushita, Department of Hematology, Nagoya University Graduate School of Medicine, 65-Tsurumai-cho, Showa-ku, Nagoya 466-8560, Japan.
Tel.: + 81 52 744 2145; fax: + 81 52 744 2161; e-mail: tmatsu@med.nagoya-u.ac.jp

Received 28 June 2005, accepted 2 September 2005

Introduction

Antithrombin (AT) is a plasma glycoprotein with a molecular weight of 58 000, one of the most important serine protease inhibitors of blood coagulation. AT inactivates thrombin and several serine proteases, including blood coagulation factors IXa, Xa, XIa, XIIa by forming a 1:1 molar complex between the active site of the serine protease and its reactive site. In the presence of heparan sulfate, the active site of the protease is brought into the close contact with the reactive site of AT, and the rate of inhibition is enhanced up to several thousand times [1–3].

Individuals deficient for AT are susceptible to venous thromboembolic diseases [4,5], but AT deficiency does not confer a predisposition to arterial thrombosis [6–8]. Nonetheless, such congenital patients are all heterozygous for its defect and individuals with an undetectable AT activity may not survive. We have generated AT-null mice through gene targeting and reported that homozygous null mice could not survive the prenatal period [9]. Extensive thrombosis occurred predominantly in the myocardium and liver sinusoids, and the embryos died before 16.5 gestational days (gd) along with massive s.c. bleeding. The skin bleeding was interpreted as arising from the consumption of coagulation factors. These results indicated the importance of AT in the anticoagulation in mouse embryo, but its organ-specific role was still unclear.

Tissue factor (TF) is a primary cellular initiator of blood coagulation. It is a transmembrane glycoprotein that binds

plasma FVII/FVIIa, that prototypically cleaves the substrates FIX and FX and initiates the coagulation protease cascade resulting in thrombin generation, fibrin deposition, and platelet activation [10,11]. TF is constitutively expressed at extravascular sites and plays an essential role in hemostasis by limiting the hemorrhage in the event of vascular injury [12].

Tissue factor is expressed during the early stages of both human and murine embryogenesis and targeted disruption of the murine TF (mTF) gene results in embryonic lethality between 9.5 and 10.5 gd [13–16]. The possible requirement of TF for embryogenesis, however, may be independent on signal transduction via TF cytoplasmic domain, as mice deficient for cytoplasmic domain are born and survive normally without any abnormalities in blood coagulation [17]. Nevertheless, prenatal lethality of complete TF deficiency in the early developmental stage appeared to limit the interpretation of TF importance in mammalian hemostasis and thrombogenesis. Previously, Parry *et al.* [18] developed transgenic mice named low TF mice ($mTF^{-/-}hTF^{+}$) and showed that fetal death could be rescued by expression of a human TF (hTF) cDNA at low levels (~1%: <0.1–1.0% of wild-type levels). The same rescuing effect was also accomplished by introducing minigenes without cytoplasmic domains. However, low TF mice had shorter life span and hemosiderin deposition and fibrosis secondary to hemorrhage of myocardium had been observed [18]. Hemodynamic studies had revealed that low TF mice had marked impairment of heart contractility [19]. These facts also suggested that TF has an pivotal role in the hemostasis of murine myocardial tissue.

The lethality of $AT^{-/-}$ embryos was because of unregulated coagulation activity and it is hypothesized that artificially reduced procoagulant activity may compensate such hemostatic unbalance. Low TF mice were crossed with $AT^{+/-}$ mice and studied whether lowering TF activity could affect the survival, and the degree of thrombosis of $AT^{-/-}$ mice. Additionally, we analyze whether bleeding in the heart of low TF mice is affected in the presence of 50% plasma AT levels that may attenuate the TF-dependent hemostasis in the heart.

Materials and methods

PCR

Each genotype was determined by PCR analyses of DNA eluted from the mouse tail. In mouse embryos, the lower limbs and tail were used. PCR for murine AT gene was performed with a forward primer (5′-CCTTCCAGACCGAACTGTCC) and a reverse primer (5′-GTAATCCCAGCCTTCTCCTG) to detect the expected deletion as previously described in Ref. [9]. For mTF gene, the PCR conditions were 33 cycles of denaturation for 1 min at 95 °C, annealing for 1 min at 65 °C, and extension for 1 min at 72 °C with a forward primer (5′-TTATAACGCACCCCGCGCCGACCCCGGC) and a reverse primer (5′-ACCGTGGGCGCGAGAGCCGCTAGGAGG). A forward primer (5′-CAAGATGGATTGCACGCAGGTTCTCC) and a reverse primer (5′-CACGAGGAAGCGGTCAGCCCATTGG) were used to detect *Neo* cassette, and a forward primer (5′-ATACATTCGAGTGCTCTGAAGTGCAT) and a reverse primer (5′-TGTTCGGGAGGGAATCACTGCTTGTTGAACA) were used for detection of hTF minigene.

Generation of AT-deficient mice with low TF activity

The generation of AT-deficient mice was described previously in Ref. [9]. Heterozygous AT-deficient mice were backcrossed to C57BL/6J congenic background for at least 10 generations. Low TF mice were generated as described earlier in Ref. [18] and transferred to Division of Experimental Animals, Center for Promotion of Medical Research and Education, Nagoya University. They have also been backcrossed to C57BL/6J. Experimental designs and protocols, including plasmid construction, generation of gene-targeting mice, were reviewed by the Nagoya University Animal Research Committee.

Strategy for breeding was summarized in Fig. 1 to generate AT-deficient mice with low TF activity. Females of low TF mice tend to suffer from the fatal bleeding complication during the gestational period. To avoid this, the female partner was set to having either $mTF^{+/+}$ or $mTF^{+/-}$ throughout the intercrossing. Here we used the notation $hTF^{+/-}$ for mice defined by breeding to contain a single copy of the human minigene and $hTF^{+/o}$ for mice that contain either one or two copies of the human minigene [20]. The first crossing was carried out between male $AT^{+/+}mTF^{-/-}hTF^{+/-}$ and female $AT^{+/-}mTF^{+/+}$ mice. Thereafter, mice heterozygous for AT and TF deficiency bearing hTF minigene, $AT^{+/-}mTF^{+/-}hTF^{+/-}$, were selected by PCR. Male or female $AT^{+/-}mTF^{+/-}hTF^{+/-}$ mice were then intercrossed and both $AT^{+/-}mTF^{-/-}hTF^{+/o}$ and $AT^{+/-}mTF^{+/-}hTF^{+/o}$ were further selected from the offsprings. Finally, pups between male $AT^{+/-}mTF^{-/-}hTF^{+/o}$ and female $AT^{+/-}mTF^{+/-}hTF^{+/o}$ mice were analyzed for the birth of pups with the expected genotypes. Thereafter, embryos of this intercrossing were collected at various times of gestation and subjected to the histological analysis (Table 1).

Two steps of intercrossing between mice bearing $hTF^{+/o}$ should result in the majority having two copies of hTF minigene both in $AT^{-/-}mTF^{+/-}hTF^{+/o}$ and $AT^{-/-}mTF^{-/-}hTF^{+/o}$. Indeed, mice were shown to have non-heterologous phenotype in terms of prenatal survival among the two genotype groups (see Results). *In vitro* studies had shown that TF activity was incomparable from the mice containing one or two copies of the minigene [20].

Histological analysis of embryos

At various times of gestation, females were sacrificed and the embryos were harvested and subjected to the histological analysis as described earlier in Refs. [9,21]. In brief, embryos were carefully dissected free of maternal tissue and a tail and a lower limb was used for genotyping by PCR analysis. Remaining tissues were washed three times in saline and fixed

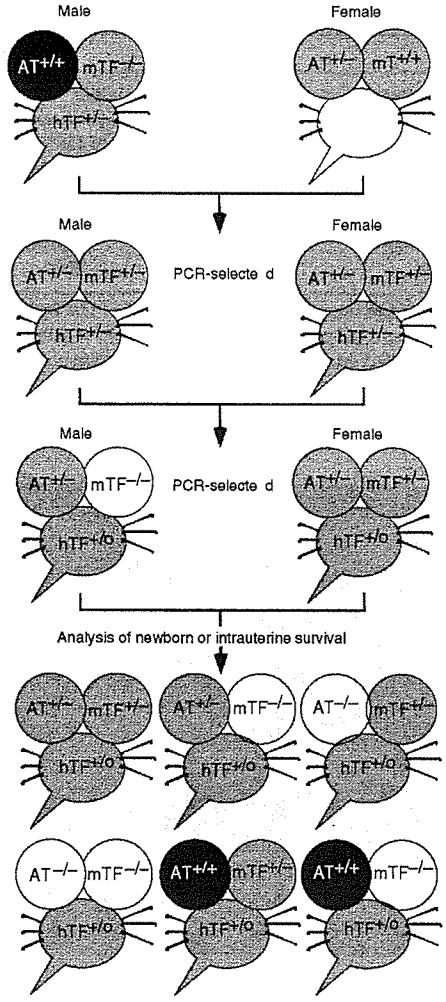

Fig. 1. Breeding strategy to generate AT-deficient mice with low TF activity. We used the notation $hTF^{+/-}$ for mice to contain a single copy of the human minigene and $hTF^{+/o}$ to contain either one or two copies of the human minigene [20] (see Materials and methods for details). Genetic status of AT, mTF, and hTF minigene was depicted in the right ear, left ear, and the face of mouse cartoon, respectively. Black-filled area denotes that both allele are present, whereas gray-shaded area denotes heterozygous status. Homozygous deficiency is represented by open white area. For status for hTF minigene, both $hTF^{+/-}$ and $hTF^{+/o}$ were denoted by gray-shaded face. To avoid bleeding complication of females with low TF, the female partner was usually set to having either $mTF^{+/+}$ or $mTF^{+/-}$. After the first crossing between male $AT^{+/+}mTF^{-/-}hTF^{+/-}$ and female $AT^{+/-}mTF^{+/+}$ mice, $AT^{+/-}mTF^{+/-}hTF^{+/-}$ was selected by the PCR and subsequently intercrossed. Finally, male $AT^{+/-}mTF^{-/-}hTF^{+/o}$ and female $AT^{+/-}mTF^{+/-}hTF^{+/o}$ mice were crossed and the birth of pups was analyzed for the six expected genotypes. Thereafter, embryos of this intercrossing were also collected and analyzed for intrauterine survival at various times of gestation (Table 1).

overnight in Carnoy's solution (methanol/chloroform/acetic acid = 6:3:1) and then dehydrated, embedded in paraffin, and sectioned (5-μm thick). Sections were stained with hematoxylin and eosin (H&E). For fibrin(ogen) immunohistochemical staining [22–24], slides were deparaffinized in xylene, transferred to 100% ethanol, and then incubated for 30 min in 0.3% H_2O_2/methanol. After rinsing with PBS, the slides were incubated successively with 5% normal goat serum/PBS (20 min, room temperature), rabbit antimouse fibrin(ogen) antibody DAKO 008 (Glostrup, Denmark; 1:200 dilution, overnight, 4 °C), antirabbit IgG Ab conjugated with biotin (1:500 dilution, 1 h, room temperature), and avidin–biotin complex conjugated with horseradish peroxidase (Vector Laboratories, Burlingame, CA, USA; 30 min, room temperature). Stained slides were visualized with diaminobenzidine tetrahydrochloride – Ni_3^+, CO_2^+ (Amersham Biosciences, Piscataway, NJ, USA).

The percent lesion of fibrin deposition was quantitated for the immunostained slides. Each pathomicrograph was scanned into a computer, and areas positive for fibrin(ogen) staining were calculated by using WinRoof, an image analysis software (Mitani Shoji, Tokyo, Japan). After establishing a color threshold, the lesion was extracted, then the percentage was calculated by dividing by the total heart or liver area. Margins or ventricular lumens of the heart were excluded from all the visual fields.

Evaluation of cardiac fibrosis

The quantitative measurement of cardiac fibrosis was according to the methods by Yoshiji, *et al.* [25]. $AT^{+/-}mTF^{-/-}hTF^{+}$ mice were analyzed according with low TF mice. Two groups were age-matched, and both were between 12 and 18 months old. The heart of sacrificed animals was quickly removed, then tissues were embedded in paraffin and stained with Azan–Mallory staining according with the control hematoxylin–eosin staining. Each pathomicrograph was scanned into a computer, and fibrotic areas positive for Azan–Mallory staining were calculated as described above. After establishing a color threshold, the blue color of the stained collagen fibers was extracted, the percentage of stained-fibers was calculated as described above.

Statistical analysis

Stat View 4.5 (SAS Institute Inc., Cary, NC, USA) was used for statistical analyses. The chi-squared tests were used to compare the distribution in each gestational age group. Student's *t*-test was used to compare the rates of myocardial fibrosis.

Results

Characterization of AT-null mice with lowered TF activity

Using targeted gene disruption, we previously generated AT-null mice and reported that 70% of $AT^{-/-}$ embryos died at 15.5 gd, while the remaining died at 16.5 gd, mainly because of hepatic and cardiac thrombosis [9]. Here we crossed $AT^{+/-}$ with low TF mice, which lack the mTF gene but contain the hTF minigene (Fig. 1), expressing ~1% TF activity [18].

Table 1 Genotypes of living embryos derived through mating between $AT^{+/-}$ $mTF^{-/-}$ $hTF^{+/o}$ and $AT^{+/-}$ $mTF^{+/-}$ $hTF^{+/o}$

Gestational day	Genotype*						
	$AT^{+/-}mTF^{+/-}$	$AT^{+/-}mTF^{-/-}$	$AT^{-/-}mTF^{+/-}$	$AT^{-/-}mTF^{-/-}$	$AT^{+/+}mTF^{+/-}$	$AT^{+/+}mTF^{-/-}$	*n*
19.5†	28 (37.3%)	13 (17.3%)	0 (0%)	4 (5.3%)	15 (20%)	15 (20%)	75
18.5	12 (27.3%)	10 (22.7%)	4 (9.1%)	7 (15.9%)	7 (15.9%)	4 (9.1%)	44
17.5	20 (33.8%)	17 (28.8%)	7 (11.9%)	3 (5.1%)	5 (8.5%)	7 (11.9%)	59
16.5	14 (38.9%)	7 (19.4%)	4 (11.1%)	3 (8.3%)	6 (16.7%)	2 (5.6%)	36
15.5	7 (21.9%)	6 (18.8%)	4 (12.5%)	4 (12.5%)	8 (25%)	3 (9.4%)	32
Expected	25%	25%	12.50%	12.50%	12.50%	12.50%	

*Genotype of each offspring is depicted without showing '$hTF^{+/o}$.' Values in parenthesis are the percentage of each birth. †The frequency of live embryos with either $AT^{-/-}mTF^{+/-}$ or $AT^{-/-}mTF^{-/-}$ was significantly smaller than the expected one in four (chi-squared $P = .0007$ for $mTF^{+/-}$ status and $P = 0.013$ for $mTF^{-/-}$ status, respectively). At other gestational days except for 19.5 gd, the observed frequencies were not different from the expected frequencies by chi-squared test.

We analyzed over three-hundred offsprings between $AT^{+/-}$ $mTF^{-/-}hTF^{+/o}$ and $AT^{+/-}mTF^{+/-}hTF^{+/o}$ mice and found that there were no living pups carrying the expected $AT^{-/-}$ genotypes; i.e. $AT^{-/-}mTF^{+/-}hTF^{+/o}$ (about 50% TF activity) or $AT^{-/-}mTF^{-/-}hTF^{+/o}$ (a trace amount of TF activity) (not shown). Therefore, even if TF activity was reduced to extremely low levels, the prenatal lethality of $AT^{-/-}$ mice could not be rescued.

To elucidate the cause of embryonic lethality, total of 246 living embryos between $AT^{+/-}mTF^{-/-}hTF^{+/o}$ and $AT^{+/-}mTF^{+/-}hTF^{+/o}$ mice were collected at various times of gestation. Living embryos were determined by their heart beating and the genotype of each embryo was determined by PCR analysis. The observed frequencies of living embryos were compared with the expected Mendelian ratios (Table 1). The PCR analysis detected hTF minigene and there were no embryos with $mTF^{-/-}hTF^{-/-}$ genotypes. We could not find the living embryos with either $AT^{-/-}$ genotypes after 20.5 gd (not shown). However, at each gestational day before 19.5 gd, the observed frequencies of all the genotypes were not statistically different from the expected frequencies by chi-squared test. At 19.5 gd, there were no $AT^{-/-}mTF^{+/-}hTF^{+/o}$ embryos and the frequency of live embryos with either $AT^{-/-}$ genotype ($AT^{-/-}mTF^{+/-}hTF^{+/o}$ and $AT^{-/-}mTF^{-/-}hTF^{+/o}$) was smaller than the expected one in four (chi-squared $P = .0007$ for $mTF^{+/-}hTF^{+/o}$ status and $P = .013$ for $mTF^{-/-}hTF^{+/o}$ status, respectively). These facts suggest that $AT^{-/-}$ embryos with reduced TF levels had longer intrauterine survival.

Dead embryos with $AT^{-/-}mTF^{+/+}$ had shown hemorrhagic skin and it was extensive s.c. hemorrhage [9]. Before 17.5 gd, there were no embryos with hemorrhagic skin, but after 17.5 gd, we also found that eight $AT^{-/-}mTF^{+/-}hTF^{+/o}$ embryos displayed hemorrhagic skin and six of them had no heart beating. Figure 2A shows live $AT^{-/-}mTF^{+/-}hTF^{+/o}$ embryos at 18.5 gd with severe s.c. hemorrhage, but no fibrin deposition was apparent by immunohistochemical staining of the whole body (data not shown). In contrast, none of dead or live $AT^{-/-}mTF^{-/-}hTF^{+/o}$ embryos exhibited s.c. hemorrhage (Fig. 2B).

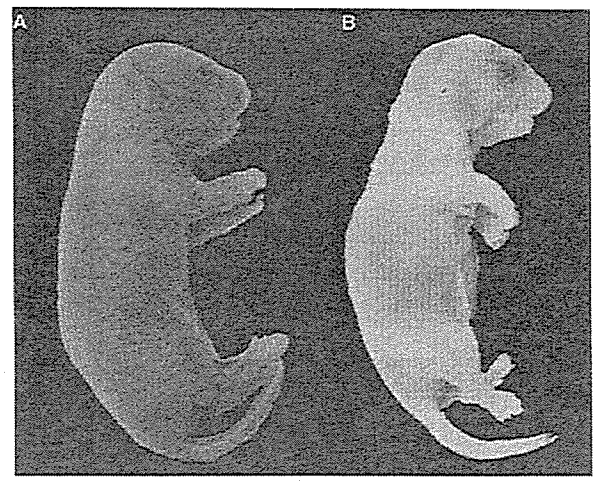

Fig. 2. Macroscopic observation of $AT^{-/-}mTF^{+/-}hTF^{+/o}$ (A) and $AT^{-/-}mTF^{-/-}hTF^{+/o}$ (B) embryos at 18.5 gd. Eight $AT^{-/-}mTF^{+/-}hTF^{+/o}$ embryos showed extensive hemorrhage between 17.5 and 19.5 gd as represented in (A) and only two were alive (see Results for detail). $AT^{-/-}mTF^{-/-}hTF^{+/o}$ embryos did not show s.c. hemorrhage (B).

Cardiac thrombosis of AT-null embryos with reduced TF activity

Mice embryos were examined histologically with H&E staining according with fibrin(ogen) immunostaining [22–24] that detects tissue fibrin deposition in various embryonal organs. Our previous findings had indicated that AT-null mice exhibited the fibrin deposition in the degenerated myocardium, beginning after 14.5 gd [9]. In $AT^{-/-}mTF^{+/-}hTF^{+/o}$, myocardial fibrin deposition was partially found from 16.5 gd (data not shown). After 16.5 gd, in all of this genotype, we found myocardial degeneration according with minor bleeding (Fig. 3A) and fibrin(ogen) immunostaining demonstrated that fibrin deposition was found in the degenerated lesion (Fig. 3B). In some embryos, large thrombi were found in the left heart auricle (Fig. 3C). The thrombi appeared to be easily formed in the left atria probably because blood flow is low in fetal

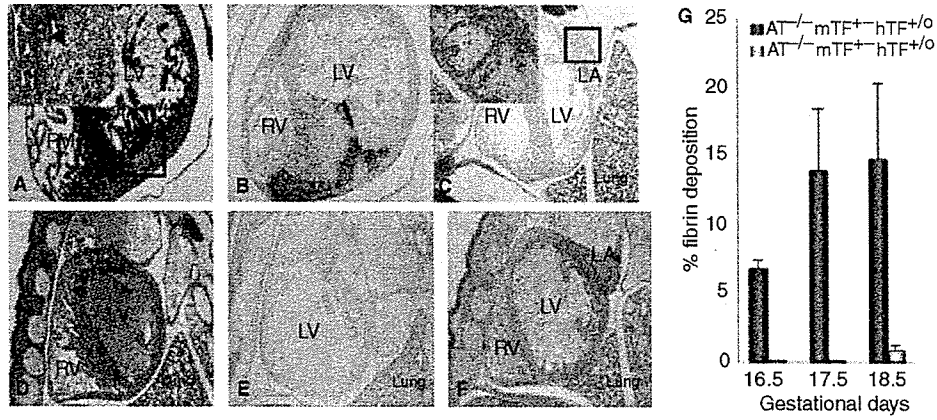

Fig. 3. Microscopic observations of embryonal myocardium. H&E staining (A, C, D, and F) or antifibrin(ogen) immunostaining (B and E) is shown for $AT^{-/-}mTF^{+/-}hTF^{+/o}$ at 17.5 gd (A–C) and $AT^{-/-}mTF^{-/-}hTF^{+/o}$ at 18.5 gd (D–F). Immunochemical staining was performed with antifibrin(ogen) antibody as described in Materials and methods. (A) Myocardial degeneration and partial necrosis were found in all of this genotype, according with the minor bleeding (◀). Inset shows high magnification of boxed area (×200). (B) Fibrin deposition, within degenerated areas, that occupies anterior, septal and partially posterior, but not lateral wall of the left ventricle. (C) A large thrombus in the left atrium (box) and is magnified in inset with ×200. (D–F) $AT^{-/-}mTF^{-/-}hTF^{+/o}$ embryos exhibit no thrombus formation in myocardium or left atrium either by H&E (D, F) or antifibrin(ogen) immunostaining (E). In panels E–F, erythrocyte pool remains in LV: left ventricle; LA: left atrium; and RV: right ventricle, while no thrombus or immunoreactive fibrin(ogen) is found. In (A)–(F), Magnification is ×40 except for inset. (G) Percent fibrin deposition was calculated as described in Materials and methods. Values are means and standard errors obtained from three living $AT^{-/-}mTF^{-/-}hTF^{+}$ or $AT^{-/-}mTF^{+/-}hTF^{+/o}$ mice at each indicated gestational day (16.5–18.5 gd). Few area of fibrin deposition were observed in $AT^{-/-}mTF^{-/-}hTF^{+/o}$ mice.

circulation. We also confirmed that atrial thrombi were found in $AT^{-/-}mTF^{+/+}$ embryos after 16.5 gd (data not shown).

Additionally, we found that the myocardial degeneration was segmental to coronary circulation. Figure 3B, for instance, indicated that fibrin deposition was formed in anterior, septal and partially posterior, but not in lateral wall of the left ventricle. Figure 4 indicated the thrombus in the small coronary vessel of living $AT^{-/-}mTF^{+/-}hTF^{+/o}$ embryo at 17.5 gd.

In contrast, the heart specimens from 21 living $AT^{-/-}mTF^{-/-}hTF^{+/o}$ embryos showed no obvious pathological abnormalities (Fig. 3D and F). Fibrin(ogen) immunostaining failed to detect the cardiac thrombosis from any specimens (Fig. 3E). We calculated the percent lesion of fibrin deposition detected by fibrin(ogen) immunostaining and found that the cardiac fibrin deposition was almost absent in $AT^{-/-}mTF^{-/-}hTF^{+/o}$ embryos (Fig. 3G). Therefore, when TF activity was abundantly lowered to ~1%, development of the cardiac thrombosis was abolished in AT-null embryos.

Liver thrombosis of AT-null embryos with reduced TF activity

$AT^{-/-}mTF^{+/+}$ also had thrombus in liver, and diffuse fibrin deposition was observed mainly in perisinusoidal space, starting from 15.5 gd [9]. There were no thrombotic changes in hepatic central veins. In the current study, both $AT^{-/-}mTF^{+/-}hTF^{+/o}$ and $AT^{-/-}mTF^{-/-}hTF^{+/o}$ embryos had similar hepatic changes and thrombi also were found in the portal veins but not in central veins (Fig. 5A–D). Figure 5E and F indicated that various extent of hepatic necrosis was observed after 15.5 gd. Figure 5G compared the degree of liver thrombosis between $AT^{-/-}mTF^{-/-}hTF^{+/o}$ and $AT^{-/-}mTF^{+/}$

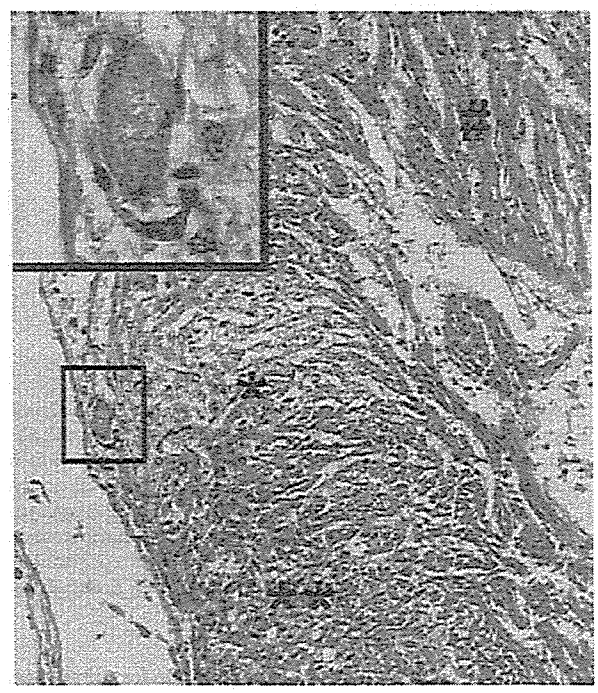

Fig. 4. Coronary thrombosis of the $AT^{-/-}mTF^{+/-}hTF^{+/o}$ embryo. A representative image of H&E staining of myocardium from $AT^{-/-}mTF^{+/-}hTF^{+/o}$ at 17.5 gd shows a thrombus in a small coronary vessel (boxed area) located in subepicardium of the left ventricular lateral wall. Magnification is ×160 and inset magnifies the boxed area with ×640. *, degenerated cardiac tissue; **, necrotic cardiac tissue; #, normal cardiomyocyte.

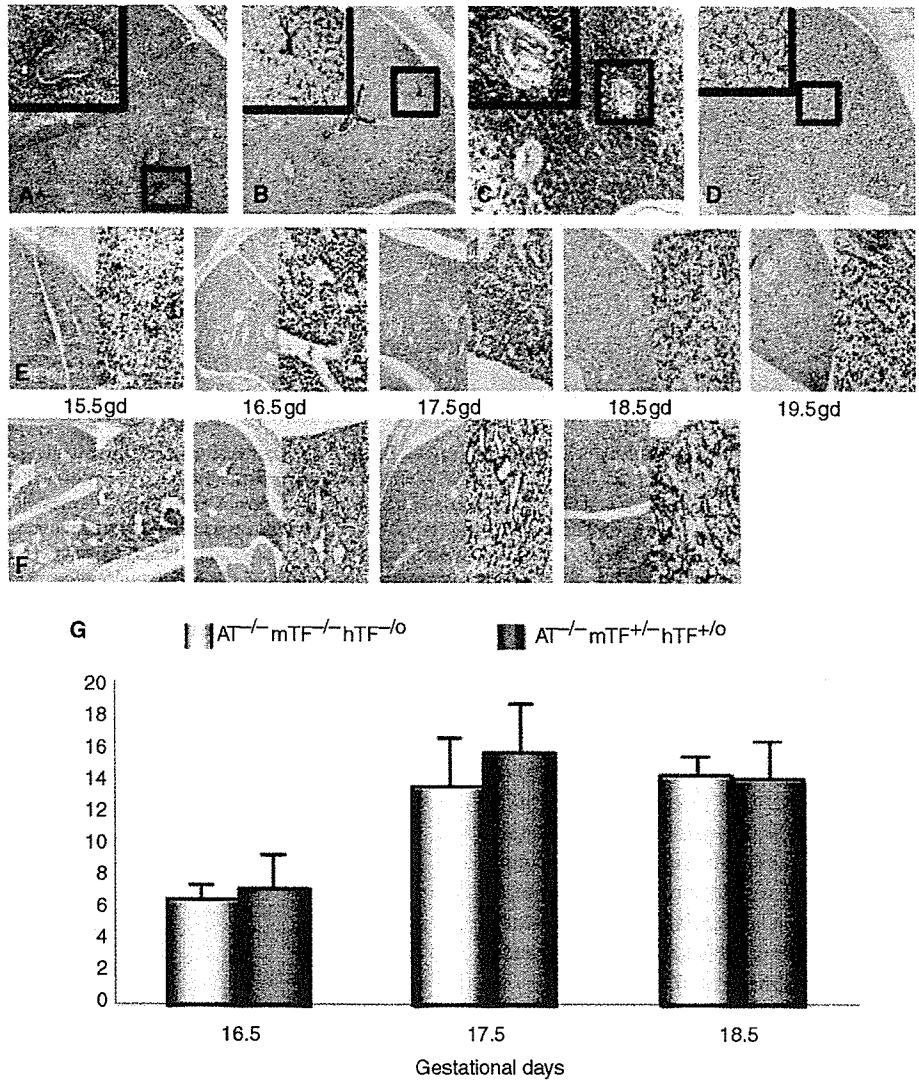

Fig. 5. Microscopic observations of the liver of $AT^{-/-}mTF^{+/-}hTF^{+/o}$ and $AT^{-/-}mTF^{-/-}hTF^{+/o}$ embryos. Panels A–D denote hepatic thrombosis in the embryo of $AT^{-/-}mTF^{-/-}hTF^{+/o}$ (A and B) or $AT^{-/-}mTF^{+/-}hTF^{+/o}$ (C and D) at 18.5 gd. H&E staining indicates large thrombus found in the intrahepatic portal vein from both genotypes (A and C). Diffuse fibrin deposition was detected in the sinusoidal space from both genotypes (B and D). Magnification: ×40. Inset magnifies boxed areas with ×200. (E and F) Time course of fibrin deposition in liver on the indicated gestational days by antifibrin(ogen) immunostaining. In E (living $AT^{-/-}mTF^{-/-}hTF^{+/o}$) and F ($AT^{-/-}mTF^{+/-}hTF^{+/o}$), each left sub-panel denotes diffuse hepatic fibrin deposition (×40 magnification) and the right sub-panel shows the close-up view of the thrombotic lesions by ×160 magnification. No embryos were living of $AT^{-/-}mTF^{+/-}hTF^{+/o}$ at 19.5 gd and were not available for the analysis. (G) The percent lesion with immunoreactive fibrin was calculated as described in the legend to Fig. 3 and compared between the liver specimen from $AT^{-/-}mTF^{-/-}hTF^{+/o}$ and $AT^{-/-}mTF^{+/-}hTF^{+/o}$. Values are means and standard errors obtained from three living $AT^{-/-}mTF^{-/-}hTF^{+}$ or $AT^{-/-}mTF^{+/-}hTF^{+/o}$ mice and no significant differences were observed at each indicated gestational day. Antifibrin(ogen) immunostaining (B, D, E, and F) was performed as described in the legend to Fig. 3.

$^{-}hTF^{+/o}$ by calculating the area positive for fibrin(ogen) immunostaining. The amount of sinusoidal fibrin deposition was the same in both genotypes and increased in intrauterine growth-dependent manner. Therefore, liver thrombosis appeared to have fatal effect both on $AT^{-/-}mTF^{+/-}hTF^{+/o}$ and $AT^{-/-}mTF^{-/-}hTF^{+/o}$. In other embryonal tissues, including brain, lung, and kidney, no fibrin deposition was detected by careful observation of immunohistochemical staining of whole body specimen (not shown).

Heterozygous AT deficiency improves cardiac fibrosis of low TF mice

Low TF mice had left ventricular dysfunction because of cardiac fibrosis that appears to be caused by minor hemorrhage, resulting in their shorter life span [19]. We also observed that cardiac fibrosis occurred in low TF mice ($AT^{+/+}mTF^{-/-}hTF^{+/o}$) and the fibrosis was extensive after 12 months old (Fig. 6A), while their littermate $AT^{+/-}mTF^{-/-}hTF^{+/o}$ showed

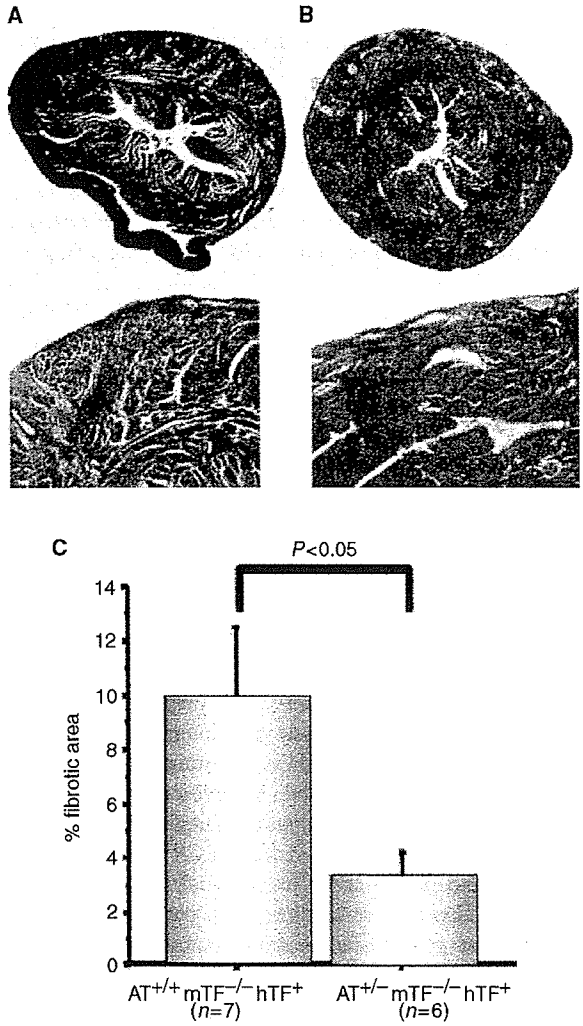

Fig. 6. Comparison of cardiac fibrosis between low TF mice and low TF mice with ~50% AT activity. Fibrotic areas were stained in blue with Azan–Mallory staining according with hematoxylin–eosin staining as described in Materials and methods. In an $AT^{+/+}mTF^{-/-}hTF^{+/o}$ mouse (low TF mice, panel A) and its littermate $AT^{+/-}mTF^{-/-}hTF^{+/o}$ (panel B) of 12 months old, horizontal section of the heart was shown by ×25 magnification (upper sub-panel) with a representative fibrotic area (lower sub-panel, ×100 magnification). (C) Percent fibrotic area was measured as described in Materials and methods, and the cardiac fibrosis is significantly decreased in $AT^{+/-}mTF^{-/-}hTF^{+/o}$ mice ($P < 0.05$). Values are means and SD obtained from 12–18-month-old $AT^{+/+}mTF^{-/-}hTF^{+/o}$ mice ($n = 7$) or their littermate $AT^{+/-}mTF^{-/-}hTF^{+}$ ($n = 6$).

decreased myocardial fibrosis (Fig. 6B). We quantitated the percent lesion of fibrosis in the assigned areas of myocardium both in 12–18-month-old $AT^{+/-}mTF^{-/-}hTF^{+/o}$ ($n = 6$) and their littermate $AT^{+/+}mTF^{-/-}hTF^{+/o}$ mice ($n = 7$). The degree of cardiac fibrosis was significantly reduced in $AT^{+/-}mTF^{-/-}hTF^{+/o}$ mice (Fig. 6C), suggesting that heterozygous for AT deficiency with ~50% AT levels protected the myocardium from fibrosis.

Discussion

Our mouse model suggest the requirement of the two procoagulant and anticoagulant proteins during the mouse development, although embryonal hemostasis may differ between various mammalian species. Previously, we observed that AT-null embryos exhibited fibrin deposition and degeneration in myocardium and liver [9]. The current study indicated that the site of thrombosis of AT-null embryos was also limited to the heart and liver. These facts suggested that AT has particular roles in the control of thrombogenesis of the two organs during mouse embryogenesis. Our analysis of over two-hundred embryos between male $AT^{+/-}mTF^{-/-}hTF^{+/o}$ and female $AT^{+/-}mTF^{+/-}hTF^{+/o}$ indicated that a reduction of TF activity failed to rescue the lethality, but prolonged the survival of AT-null embryos by several days (Table 1).

We examined the hearts from the total of 21 embryos of AT-null with low TF activity ($AT^{-/-}mTF^{-/-}hTF^{+/o}$) and no pathological abnormality was detected (Fig. 3), indicating that reduction of TF activity to extremely low levels could relieve from the cardiac thrombosis, whereas about 50% reduction could not (Fig. 3). Apparently, in the heart, hypercoagulable state of AT-null embryos appeared to be balanced by the absence of TF-initiated activation of coagulation proteases. In our timed mating, no embryos could be produced with $AT^{-/-}mTF^{+/+}$ but the comparison with our previous observation suggested that the occurrence of cardiac thrombosis appeared to delay in 1–2 days in $AT^{-/-}mTF^{+/-}hTF^{+/o}$ mice. We also found four living embryos with $AT^{-/-}mTF^{-/-}hTF^{+/o}$ at 19.5 gd. It is therefore possible that the delayed or absence of cardiac thrombosis and degeneration might benefit the slight life prolongation of AT-null embryos.

In $AT^{-/-}mTF^{+/-}hTF^{+/o}$ embryos, thrombi were found in small coronary arteries (Fig. 4) and the pattern of fibrin deposition was segmental to irrigation by the coronary artery flow (Fig. 3B), suggesting that the complete AT deficiency may lead to thrombus formation in cardiac vessels followed by ischemic myocardial damage. Previously, several studies of ischemia-reperfusion (I/R) injury models of adult animals had found the increased TF activity [26] or increased TF mRNA, antigen, and activity [27], suggesting that ischemic damage results in higher TF expression in cardiomyocytes. Also, damage to the endothelial barrier would permit the plasma clotting factors to gain access to TF expressed by the extravascular cardiomyocytes, probably leading to local thrombin generation and fibrin deposition. We also observed myocardial degeneration according to bleeding, and thus fibrin deposition might also have in part resulted from microvascular bleeding in degenerated myocardium. Therefore, AT would have been needed to protect from the unregulated thrombin generation, and probably from the fibrin deposition in the myocardium of AT-null mice. At present, however, thrombi were found only in middle-smaller-sized vessels and it is not determined whether larger coronary arteries were affected as in conventional myocardial infarction of human adults.

In turn, the principal role of TF in the hemostasis of the heart has been suggested by the fact that the heart from elderly low TF mice had shown extensive fibrosis secondary to the hemorrhage of myocardium [19]. Interestingly, our experiment indicated that the fibrosis of low TF mice was significantly decreased by heterozygous AT deficiency (Fig. 6). Thus, our current study suggest that AT anticoagulation system is fitted to hemostatic balance of the murine heart in terms of counterbalancing of the TF-initiated thrombin generation.

Unlike our intercrossing between AT-null and low TF mice, another intercrossing resulted in the successful rescue of lethality of mice deficient for a potent anticoagulant. Mice deficient for TFPI suffered from disseminated thrombosis and are embryonic lethal apparently because of the intracranial hemorrhage [28]. Crossbreeding with low TF mice completely rescued the lethal thrombogenesis of TFPI-null mice [20], demonstrating its role as a specific antagonist of TF-initiated coagulation. In turn, decreases in TFPI levels did not rescue the fibrotic myocardium followed by the repeated hemorrhagic events of low TF mice [20], presenting a good contrast with our finding. Such difference is in part dependent on possibly distinct magnitude of anticoagulant roles of the two proteins in the heart, nonetheless which is totally unknown. At least, unlike AT-null mice, cardiac thrombosis has not been described in TFPI-null mice [28] and TFPI may have less important roles in antithrombogenesis in the murine heart.

By contrast to the findings in the heart, hepatic thrombus formation and necrosis were observed by the gestational age-dependent manner from AT-null mice having either TF genotype (Fig. 5). In embryonal circulation, the portal system is connected to the umbilical artery and placenta. Fibrin deposition was detected in liver sinusoids, but not in the central veins (Fig. 5A–D), therefore, thrombosis in the portal system might cause severe hepatic dysfunction of the embryos. Thus, development of massive liver thrombosis may be critical for life of the embryos.

In $AT^{-/-}mTF^{-/-}hTF^{+/o}$ embryos, the marked difference of occurrence of thrombosis between the heart and liver remains unexplained. However, a study compared sodium dodecyl sulphate (SDS)-soluble extracts of various human organs and found that AT is predominated in liver compared with other organs [29]. AT acts more efficiently in the presence of heparan sulfate and thus AT deficiency might be profound in the organ that is rich in endothelium-based heparan sulfate proteoglycan. Indeed, heparan sulfate exhibits an unusually high degree of sulfation from the liver compared with other tissues, that is crucial for interaction with AT [30]. In this context, guard from thrombogenesis may be more dependent on AT that tightly associates with heparan sulfate of the hepatic vascular bed.

Liver is composed by various cell types including Kupfer cells that predominantly express TF on its cell surface. However, low TF mice did not have the bleeding in the liver and mTF mRNA expression was lower in the liver than in the heart [18], although it is not known whether liver is insignificant for TF-dependent activation of coagulation cascades. In this situation, differences in TF impact on liver thrombogenesis might result in different rescue of thrombosis in AT-null mice, although the entire reasons should need further studies including careful observation of spatial distribution of cellular TF.

We had observed that all the dead $AT^{-/-}mTF^{+/+}$ embryos had shown extensive s.c. hemorrhage [9], but we could find that only eight embryos (two living) showed skin hemorrhage with $AT^{-/-}mTF^{+/-}hTF^{+/o}$ genotype. Because we observed that most of the living embryos did not show skin hemorrhage, it might occur at the critical period of death and the hemorrhage is probably not necessarily related to the cause of death. Interestingly, skin hemorrhage was not found in $AT^{-/-}mTF^{-/-}hTF^{+/o}$ at any gestational ages (Fig. 2B), suggesting that the hemorrhage appeared to be attenuated by lowering the TF levels. Currently, we have found no fibrin deposition subcutaneously from any mouse genotypes (not shown), and the consumption of coagulation factors may underlie the s.c. hemorrhage because of massive thrombus formation. Absolutely, it could not be measured whether fibrinogen or other coagulation factors were decreased in the embryonal plasma and the cause of the s.c. hemorrhage is not entirely determined.

Authorship details

Mutsuharu Hayashi: tissue section preparation and HE staining, writing, data analysis and interpretation; Tadashi Matsushita: data interpretation and writing; Nigel Mackman: low TF mice provision and supervision of manuscript; Masafumi Ito: fibrinogen immunostaining and interpretation of organ pathology; Tatsuya Adachi: PCR analysis of mouse tail DNA and plaque check plus general mice maintenance; Kyosuke Takeshita: instruction of experimentation (MH) especially for general animal manipulation and PCR; Koji Yamamoto: PCR analysis of mouse tail DNA; Akira Katsumi: statistical analysis, supervision and manuscript revision; Tetsuhito Kojima: PCR Primer design and writing; Hidehiko Saito: conception of project and supervision; Toyoaki Murohara and Tomoki Naoe: coordination of project and manuscript writing.

Acknowledgements

This work was supported in part by grants-in-aid No. 16590933 from Japan Society for the Promotion of Science (TM), and also from the Japanese Ministry of Health, Labor and Welfare (TK). We especially give many thanks to Dr Masamitsu Yanada for his corporations and helpful advices. We thank Keiko Kinoshita, Tomoyo Nezu, Makoto Ikejiri, Takayuki Yamada, and Takashi Iwasaki for their excellent technical assistance.

References

1 Bauer KA, Rosenberg RD. Role of antithrombin III as a regulator of in vivo coagulation. *Semin Hematol* 1991; **28**: 10–8.
2 Blajchman MA, Austin RC, Fernandez-Rachubinski F, Sheffield WP. Molecular basis of inherited human antithrombin deficiency. *Blood* 1992; **80**: 2159–71.

3 Pratt CW, Church FC. Antithrombin: structure and function. *Semin Hematol* 1991; **28**: 3–9.
4 Lane DA, Kunz G, Olds RJ, Thein SL. Molecular genetics of antithrombin deficiency. *Blood Rev* 1996; **10**: 59–74.
5 Bayston TA, Lane DA. Antithrombin: molecular basis of deficiency. *Thromb Haemost* 1997; **78**: 339–43.
6 Greaves M, Preston FE. The hypercoagulable state in clinical practice. *Br J Haematol* 1991; **79**: 148–51.
7 Thomas DP, Roberts HR. Hypercoagulability in venous and arterial thrombosis. *Ann Intern Med* 1997; **126**: 638–44.
8 De Stefano V, Finazzi G, Mannucci PM. Inherited thrombophilia: pathogenesis, clinical syndromes, and management. *Blood* 1996; **87**: 3531–44.
9 Ishiguro K, Kojima T, Kadomatsu K, Nakayama Y, Takagi A, Suzuki M, Takeda N, Ito M, Yamamoto K, Matsushita T, Kusugami K, Muramatsu T, Saito H. Complete antithrombin deficiency in mice results in embryonic lethality. *J Clin Invest* 2000; **106**: 873–8.
10 Edgington TS, Mackman N, Brand K, Ruf W. The structural biology of expression and function of tissue factor. *Thromb Haemost* 1991; **66**: 67–79.
11 Nemerson Y. Tissue factor and hemostasis. *Blood* 1988; **71**: 1–8.
12 Drake TA, Morrissey JH, Edgington TS. Selective cellular expression of tissue factor in human tissues. Implications for disorders of hemostasis and thrombosis. *Am J Pathol* 1989; **134**: 1087–97.
13 Luther T, Flossel C, Mackman N, Bierhaus A, Kasper M, Albrecht S, Sage EH, Iruela-Arispe L, Grossmann H, Strohlein A, Zhang Y, Nawroth PP, Carmeliet P, Loskutoff DJ, Muller M. Tissue factor expression during human and mouse development. *Am J Pathol* 1996; **149**: 101–13.
14 Toomey JR, Kratzer KE, Lasky NM, Stanton JJ, Broze Jr GJ. Targeted disruption of the murine tissue factor gene results in embryonic lethality. *Blood* 1996; **88**: 1583–7.
15 Bugge TH, Xiao Q, Kombrinck KW, Flick MJ, Holmback K, Danton MJ, Colbert MC, Witte DP, Fujikawa K, Davie EW, Degen JL. Fatal embryonic bleeding events in mice lacking tissue factor, the cell-associated initiator of blood coagulation. *Proc Natl Acad Sci USA* 1996; **93**: 6258–63.
16 Carmeliet P, Mackman N, Moons L, Luther T, Gressens P, Van Vlaenderen I, Demunck H, Kasper M, Breier G, Evrard P, Muller M, Risau W, Edgington T, Collen D. Role of tissue factor in embryonic blood vessel development. *Nature* 1996; **383**: 73–5.
17 Melis E, Moons L, De Mol M, Herbert JM, Mackman N, Collen D, Carmeliet P, Dewerchin M. Targeted deletion of the cytosolic domain of tissue factor in mice does not affect development. *Biochem Biophys Res Commun* 2001; **286**: 580–6.
18 Parry GC, Erlich JH, Carmeliet P, Luther T, Mackman N. Low levels of tissue factor are compatible with development and hemostasis in mice. *J Clin Invest* 1998; **101**: 560–9.
19 Pawlinski R, Fernandes A, Kehrle B, Pedersen B, Parry G, Erlich J, Pyo R, Gutstein D, Zhang J, Castellino F, Melis E, Carmeliet P, Baretton G, Luther T, Taubman M, Rosen E, Mackman N. Tissue factor deficiency causes cardiac fibrosis and left ventricular dysfunction. *Proc Natl Acad Sci USA* 2002; **99**: 15333–8.
20 Pedersen B, Holscher T, Sato Y, Pawlinski R, Mackman N. A balance between tissue factor and tissue factor pathway inhibitor is required for embryonic development and hemostasis in adult mice. *Blood* 2005; **105**: 2777–82.
21 Yanada M, Kojima T, Ishiguro K, Nakayama Y, Yamamoto K, Matsushita T, Kadomatsu K, Nishimura M, Muramatsu T, Saito H. Impact of antithrombin deficiency in thrombogenesis: lipopolysaccharide and stress-induced thrombus formation in heterozygous antithrombin-deficient mice. *Blood* 2002; **99**: 2455–8.
22 Wilhelm O, Hafter R, Coppenrath E, Pflanz MA, Schmitt M, Babic R, Linke R, Gossner W, Graeff H. Fibrin-fibronectin compounds in human ovarian tumor ascites and their possible relation to the tumor stroma. *Cancer Res* 1988; **48**: 3507–14.
23 Moons L, Shi C, Ploplis V, Plow E, Haber E, Collen D, Carmeliet P. Reduced transplant arteriosclerosis in plasminogen-deficient mice. *J Clin Invest* 1998; **102**: 1788–97.
24 Wang J, Zheng H, Ou X, Albertson CM, Fink LM, Herbert JM, Hauer-Jensen M. Hirudin ameliorates intestinal radiation toxicity in the rat: support for thrombin inhibition as strategy to minimize side-effects after radiation therapy and as countermeasure against radiation exposure. *J Thromb Haemost* 2004; **2**: 2027–35.
25 Yoshiji H, Buck TB, Harris SR, Ritter LM, Lindsay CK, Thorgeirsson UP. Stimulatory effect of endogenous tissue inhibitor of metalloproteinases-1 (TIMP-1) overexpression on type IV collagen and laminin gene expression in rat mammary carcinoma cells. *Biochem Biophys Res Commun* 1998; **247**: 605–9.
26 Golino P, Ragni M, Cirillo P, Avvedimento VE, Feliciello A, Esposito N, Scognamiglio A, Trimarco B, Iaccarino G, Condorelli M, Chiariello M, Ambrosio G. Effects of tissue factor induced by oxygen free radicals on coronary flow during reperfusion. *Nat Med* 1996; **2**: 35–40.
27 Chong AJ, Pohlman TH, Hampton CR, Shimamoto A, Mackman N, Verrier ED. Tissue factor and thrombin mediate myocardial ischemia-reperfusion injury. *Ann Thorac Surg* 2003; **75**: S649–55.
28 Huang ZF, Higuchi D, Lasky N, Broze Jr GJ. Tissue factor pathway inhibitor gene disruption produces intrauterine lethality in mice. *Blood* 1997; **90**: 944–51.
29 Kamp P-B, Strathmann A, Ragg H. Heparin cofactor II, antithrombin-[beta] and their complexes with thrombin in human tissues. *Thromb Res* 2001; **101**: 483.
30 Lyon M, Deakin JA, Gallagher JT. Liver heparan sulfate structure. A novel molecular design. *J Biol Chem* 1994; **269**: 11208–15.

Haemophilia (2006), 12, 172–178 DOI: 10.1111/j.1365-2516.2006.01206.x

CASE REPORT

A case of coagulation factor V deficiency caused by compound heterozygous mutations in the factor V gene

N. YAMAKAGE,* M. IKEJIRI,* K. OKUMURA,* A. TAKAGI,*† T. MURATE,*† T. MATUSHITA,‡ T. NAOE,‡ K. YAMAMOTO,§ J. TAKAMATSU,§ T. YAMAZAKI,¶ M. HAMAGUCHI¶ and T. KOJIMA*†

**Department of Pathophysiological Laboratory Sciences, Nagoya University Graduate School of Medicine; †Department of Medical Technology, Nagoya University School of Health Sciences; ‡Department of Hematology, Nagoya University Graduate School of Medicine; §Division of Transfusion Medicine, Nagoya University Hospital; and ¶Department of Hemostatis and Thrombosis Clinical Research Center, National Hospital Organisation, Nagoya Medical Center, Nagoya, Japan*

Summary. We investigated the molecular basis of a severe factor V (FV) deficiency in a Japanese female, and identified two distinct mutations in the FV gene, a novel cytosine insertion (1943insC) and a previously reported point mutation (A5279G). We expected the patient to be a compound heterozygote for those mutations, as a 1943insC, but not an A5279G, was found in the mother and a sibling. The 1943insC will cause a frame-shift after ^{590}Gln, resulting in amino acid substitutions with two abnormal residues followed by a stop codon in the FV A2 domain (FS592X). The A5279G will cause an amino acid alteration in the FV A3 domain (Y1702C), which has been observed in several ethnic groups. We found that both mutant mRNAs were detected by reverse transcriptase polymerase chain reaction (RT-PCR) in the patient's platelets, whereas no FV antigen and activity were detected in plasma. On the one hand, the RT-PCR signal from the FS592X-FV mutant mRNA was markedly reduced, suggesting that the RNA surveillance system would eliminate most of the abnormal FS592X-FV transcripts with a premature termination. On the other hand, expression analyses revealed that only small amounts of Y1702C-FV with a low specific activity were secreted, and that the FS592X-FV was not detected in cultured media. These data indicated that both mutant FV molecules would be impaired, at least in part, during the post-transcriptional process of protein synthesis and/or in secretion. Taken together, it seems to suggest that each gene mutation could be separately responsible for severe FV deficiency, while this phenotype is due to the in-trans combination of the two defects.

Keywords: compound heterozygote, expression study, factor V deficiency, gene mutation, parahaemophilia, reverse transcriptase polymerase chain reaction

Introduction

Human coagulation factor V (FV) is a large (molecular weight of 330 kDa) single-chain glycoprotein that circulates in blood as an inactive procoagulant cofactor and plays an important role in the blood coagulation cascade [1,2]. The cDNA clones encoding human FV have been isolated [3], and the human FV gene has been mapped to chromosome 1q23 and spans approximately 80 kb of DNA [4]. The human FV gene consists of 25 exons and 24 introns, and the mRNA encodes 2224-amino acid protein containing a leader peptide of 28 amino acids [5]. It is comprised of three homologous A-type domains, two homologous C-type domains, and a heavily glycosylated B domain and shows a linear domain structure (A1-A2-B-A3-C1-C2) homologous to factor VIII (FVIII) with 35–40% homology existing in both the A-type and C-type domains [1,2]. Thrombin activates FV by the proteolytic release of the B domain, resulting in the formation of a non-covalently bound heterodimeric molecule of the heavy chain (residues 1–709, A1-A2 domains) and

Correspondence: Tetsuhito Kojima, MD, PhD, Professor, Department of Pathophysiological Laboratory Sciences, Nagoya University Graduate School of Medicine, 1-1-20 Daiko-Minami, Higashi-ku, Nagoya 461-8673, Japan.
Tel.: 81 52 719 3153; fax: 81 52 719 3153;
e-mail: kojima@met.nagoya-u.ac.jp

Accepted after revision 7 December 2005

light chain (residues 1546–2196, A3-C1-C2 domains), activated FV (FVa) [6].

Activated FV functions as an essential molecule of the prothrombinase complex that catalyses the conversion of prothrombin to thrombin by factor Xa in the presence of calcium and a phospholipid membrane. The procoagulant function of FVa is downregulated by the anticoagulant serine protease, an activated protein C (APC) [7] that cleaves to FVa at Arg306, Arg506 and Arg679, resulting in a loss of FVa activity. On the other hand, FV cleaved by APC before thrombin activation, FVac, shows an anticoagulant function as a cofactor in the APC-mediated inactivation of activated FVIII (FVIIIa). Thus, FV plays an important role in the procoagulant pathway as well as in the protein C anticoagulant pathway [8].

Around 75% of FV in blood is in the plasma, with the residual FV in the α-granules of blood platelets. In plasma, FV exists in two isoforms (FV1 and FV2) that have different molecular weights because of partial N-linked glycosylation in the C2 domain [9]. FV1 and FV2 have different characteristics in terms of procoagulant activity, inactivation by APC, and their anticoagulant function in the protein C pathway [10]. Consequently, FV1 has the overall potential to generate more thrombin than FV2.

Factor V deficiency, also known as parahaemophilia, was first described in 1947 by Owren [11]. It is a rare bleeding disorder inherited in an autosomal recessive manner with an incidence of about one in 1 million [1]. Bleeding symptoms in FV-deficient patients are varied; heterozygotes are usually asymptomatic, whereas homozygotes may show a mild, moderate or severe bleeding tendency.

To date, more than 40 identified cases of mutations in the FV gene were described in FV-deficient patients in the homozygous or compound heterozygous state [12]. In this study, we investigated the molecular basis of severe FV deficiency in a Japanese patient, and demonstrated that she was another compound heterozygote for FV gene mutations resulting in the post-transcriptional impairment of FV synthesis and/or secretion.

Materials and methods

Preparation of plasma, genomic DNA and total RNA of platelets

Ethical approval for the study was obtained from the Ethics Committee of the Nagoya University School of Medicine. Following informed consent, blood samples from the patient, family members and volunteers were collected in a 1:10 volume of 3.13% sodium citrate. Plasma was separated by centrifugation at 2000 *g* for 20 min, and aliquots were stored at −70°C until use. The patient had not received substitution therapy for 3 months prior to blood sampling for FV antigen and activity measurements. Genomic DNA was isolated from peripheral blood leucocytes as described previously [13]. Citrated blood samples from the patient and her sibling were centrifuged at 250 *g* for 5 min at 4°C to collect platelet-rich plasma. Subsequently, the total RNA was extracted from platelets by RNA STAT-60 (Tel-Test Inc., Friendswood, TX, USA), and subjected to a reverse transcription (RT) reaction as described below.

FV antigen and activity assays

Factor V procoagulant activity and FV antigen in plasma as well as in culture media containing recombinant FV proteins were measured as described below. FV procoagulant activity was measured by one-stage clotting assay, of which the sensitivity limit and the normal range are 3% and 70–135%, respectively, using human FV-deficient plasma (George King Bio-Medical, Overland, KS, USA) and Simplastin (Biomerieux, Inc., Durham, NC, USA). FV antigen was measured by enzyme-linked immunosorbent assay (ELISA), of which the sensitivity limit and the normal range are 1% and 70–135%, respectively, using an affinity-purified sheep anti-human FV IgG as a coating antibody with a peroxidase-conjugated sheep anti-FV antibody as a second antibody, according to the manufacturer's protocol (Cedarlane Lab. Ltd, Hornby, ON, Canada). In both assays, FV levels were expressed as a percentage of control plasma pooled from 25 healthy individuals.

PCR and DNA sequencing

The polymerase chain reaction (PCR) primers were synthesized to amplify all exons and splicing junctions of the FV gene, based on the reported genomic DNA sequence of human FV (GenBank Z99572). Information of the primer sequences is available from the authors. PCR amplification of the FV gene was performed with rTaq polymerase or exTaq polymerase (Takara Bio Inc., Kusatsu, Japan) in 30–35 cycles under the following conditions: 30 s denaturing at 94°C, 30 s annealing at 47–58°C and 30 s extension at 72°C.

Polymerase chain reaction products were separated by agarose gel electrophoresis, and authentic fragments were collected and purified with a QUAEX II kit (Qiagen K.K., Tokyo, Japan). The samples were then directly sequenced by a Big Dye Terminator

Cycle Sequencing FS Ready Reaction kit (Applied Biosystems, Foster City, CA, USA) using forward or reverse PCR primers, according to the manufacturer's protocol. The sequencing products were then precipitated with 0.15 M NaOAc (pH 8.0) and cold ethanol, washed once with 70% ethanol, dried, resuspended in 25 μL of Template Suspension Reagent (Applied Biosystems), and analysed by an ABI Prism 310 Genetic Analyzer (Applied Biosystems).

Analysis of FV mRNA

To investigate the presence of FV transcripts from the mutant allele in platelets, we analysed platelet RNAs from the proband by mRNA-based PCR-restriction fragment length polymorphisms (RFLPs). In brief, total RNA extracted from the platelets was reverse-transcribed using the respective gene-specific primers: 12GSP (5′-TCTGTTCTGGTAATCA TAGT-3′) for 1943insC or 15GSP (5′-GTGCTG TTTATTGCCATTTT-3′) for A5279G, and Super Script II RT reverse transcriptase (Invitrogen Japan, Tokyo, Japan). To detect the 1943insC mutation, a nested PCR was performed using the following primers: 12rPCR-UP (5′-CCCTATAGCATTTAC CCTCA-3′) and 12GPS for the first PCR, and 12mut-UP (5′-ACTTCTGTAGTGTGGGGggCC-3′; bold lower case characters are mismatched nucleotides) and 12 M-LW (5′-TTCATCATCATCTGGG-ATAC-3′) for the second PCR, introducing a new *Apa*I restriction site in the mutant PCR products, as a single PCR using the first or second PCR primer set failed to amplify authentic PCR products. The 1943insC mutant RT-PCR products would yield 19- and 221-bp fragments, whereas the wild-type products would not be digested (239 bp). To detect the A5279G mutation, PCR was performed with the following primers: 15 M-UP (5′-AAAAATCATCA GAGGGAAAG-3′) and 15mut-LW (5′-CTGGGT TCACAGCTGAcTAG-3′) introducing a *Spe*I restriction site in the wild-type PCR products. Thus, the wild-type RT-PCR products would yield 18- and 159-bp fragments, while the A5279G mutant products would not be digested (177 bp). These fragments were run on a 4% agarose gel and stained with ethidium bromide. We evaluated the allele-specific mRNA levels by the quantitative densitometric analyses using the NIH image software (version 1.62) (National Institutes of Health, Bethesda, MD, USA).

Preparation of mutant FV expression vectors

We prepared individual FV expression vectors bearing the identified mutations, 1943insC (FS592X; the initial Met residue is denoted amino acid +1) and A5279G (Y1702C), based on pMT2 containing a full-length cDNA of human FV (pMT2-FV). Both mutations were introduced individually into the pMT2-FV expression vector using the recombinant PCR method described elsewhere [14]. After recombinant PCRs, each DNA fragment encoding the 1943insC or A5279G mutation was isolated as *Bsp*36I-*Bsp*EI or *Bsp*MI-*Sna*BI fragments, and separately replaced into the appropriate position for the pMT2/FV expression vector. DNA sequencing confirmed that no unexpected mutation was found in any of the whole mutant inserts in either construct.

Transient expression of recombinant FVs in COS-1 cells

African green monkey kidney COS-1 cells were cultured in a 5% CO_2 humidified atmosphere at 37°C in Dulbecco modified Eagle medium (DMEM; Invitrogen) supplemented with fetal calf serum (10%), glutamine (1%), and antibiotics (penicillin and streptomycin, 100 IU mL^{-1} and 100 μg mL^{-1} respectively). Cells in 30-mm dishes were transfected with either wild type or individual mutant plasmids using the Fu-GENE6™ transfection reagent (Roche Diagnostics K.K., Tokyo, Japan) according to the manufacturer's instructions. After 48-h culture of the transfected cells in serum-free DMEM, conditioned media containing the secreted recombinant proteins were collected, then concentrated using Centrisart I (cut off MW 20000; Sartorius, Goettingen, Germany), and subjected to one-stage clotting assay as well as ELISA (Cedarlane Lab. Ltd) for recombinant FV antigen measurements as described above.

Results and discussion

Case report

The patient (individual II-1, Fig. 1) is a 39-year-old Japanese woman who had recurrent episodes of bleeding such as epistaxis, joint region haematoma and hypermenorrhea, which were treated with FV replacement therapy by transfusion of fresh frozen plasma. When the patient was 4 years old, she had been diagnosed as having coagulation FV deficiency, since laboratory tests revealed that the prothrombin time and the activated partial thromboplastin time were prolonged, and FV activity was below the measurable limit. There was no history of bleeding tendencies in her other family members tested, since FV activities in plasma of both her mother and a sibling were 65%, suggesting that they might be

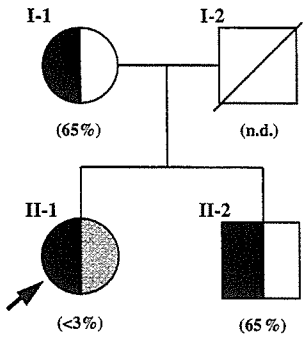

Fig. 1. Pedigree of the factor V-deficient family. The propositus is subject II-1 (arrow). Circle and square indicates male and female respectively. Values in parentheses represent plasma factor V activities (n.d., not done). Subjects with 1943insC and A5279G mutations are demonstrated with solid and shaded areas respectively.

heterozygous for FV-deficiency causing mutation. Consanguinity in the family was excluded.

DNA sequencing

In order to identify causative FV gene mutation(s) in such an FV-deficient patient, we analysed nucleotide sequences of all 25 exons and exon–intron boundaries of the FV gene. Results from direct sequencing of the FV gene revealed that the patient had a C insertion in three consecutive cytosine nucleotides [^{589}Thr(ACC)–^{590}Gln(CAG)] in exon 12 at nucleotide positions 1940–1942 (1943insC), and an A–G transition in exon 15 at nucleotide position 5279 (A5279G) (Fig. 2). DNA samples from her mother and brother also showed heterozygosity for the 1943insC mutation, but no A5279G mutation (data not shown), which are consistent with the data of plasma FV activity, i.e. about half that of normal subjects; 1943insC is a novel mutation, which can cause a frame-shift resulting in a substitution of the amino acids after ^{590}Gln with two abnormal residues (^{590}Pro–^{591}Glu) followed by a stop codon (FS592X). The A5279G will cause the amino acid substitution Y1702C, which was previously designated FV Seoul 2 [15]. The A5279G FV gene mutation has also been found in Italian and Slovenian subjects [16,17], and is thought to be a very ancient and/or recurrent mutation. In this study, we demonstrated that this mutation also occurred in a Japanese subject, suggesting that the A5279G might be a hot-spot mutation rather than a founder mutation.

mRNA analysis (RT-PCR RFLPs)

We analysed the expression of mutant FV gene transcripts from the patient's platelets by mRNA-mediated PCR-RFLPs (RT-PCR RFLPs). For 1943insC (FS592X-FV mRNA), the nested RT-PCR followed by *Apa*I digestion yielded 239- and 221-bp bands, representing transcripts from the normal and mutant alleles, respectively, although the mutant signal was markedly reduced (Fig. 3a). For A5279G (Y1702C-FV mRNA), the RT-PCR products digested with *Spe*I yielded 159- and 177-bp bands, representing transcripts from the normal and mutant alleles respectively (Fig. 3b). Thus, both mutant transcripts were present in the patient's platelets. However, the FS592X-FV mRNA signal was markedly reduced to 12% of the wild type in the quantitative densitometric analysis, whereas the Y1702C-FV mRNA signal was more intense (250% of the wild type). These data suggest that the patient could be compound heterozygous for these mutations, and that her RNA surveillance system would eliminate most of the FV mRNA derived from the mutant allele encoding a premature termination by the frame-shift mutation, FS592X [18]. On the other

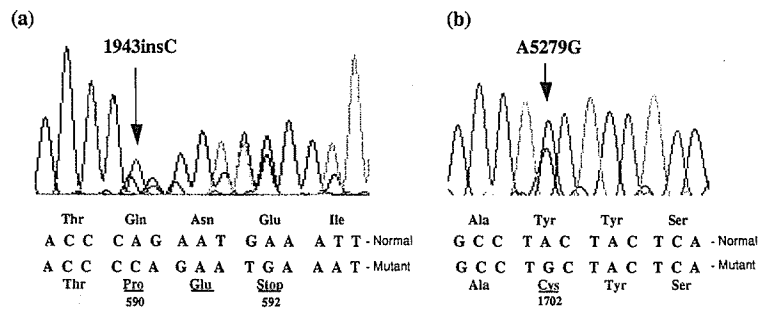

Fig. 2. Patient's nucleotide and amino acid sequences surrounding the mutations. (a) Nucleotide and amino acid sequences surrounding 1943insC. Arrow indicates mutation point. The mutation predicts an abnormal sequence of two amino acid residues and a stop codon. (b) Nucleotide and amino acid sequences surrounding A5279G. Arrow denotes mutation point. Patient's heterozygous sequencing pattern is shown.